Evaluating Continual Learning on a Home Robot

Sam Powers
Robotics Institute
Carnegie Mellon University
snpowers@cs.cmu.edu

Abhinav Gupta
Robotics Institute
Carnegie Mellon University
abhinavg@cs.cmu.edu

Chris Paxton
Meta AI
cpaxton@meta.com

Abstract

Robots in home environments need to be able to learn new skills continuously as data becomes available, becoming ever more capable over time while using as little real-world data as possible. However, traditional robot learning approaches typically assume large amounts of iid data, which is inconsistent with this goal. In contrast, continual learning methods like CLEAR and SANE allow autonomous agents to learn off of a stream of non-iid samples; they, however, have not previously been demonstrated on real robotics platforms. In this work, we show how continual learning methods can be adapted for use on a real, low-cost home robot, and in particular look at the case where we have extremely small numbers of examples, in a task-id-free setting. Specifically, we propose SANER, a method for continuously learning a library of skills, and ABIP (Attention-Based Interaction Policies) as the backbone to support it. We learn four sequential kitchen tasks on a low-cost home robot, using only a handful of demonstrations per task.

1 Introduction

For a home robot to be fully capable, it must be able to adapt to the changing needs of the home. If a new appliance is purchased, the robot should be able to learn to use it seamlessly, without forgetting any previous skills it has learned. If new storage is purchased, the robot should be able to utilize previous knowledge it has about putting objects away to quickly learn to leverage it. Since no two homes, or humans, are the same, it is not feasible to rely entirely upon pre-training in controlled settings to enable a robot to do everything that might be asked of it.

In other words, we see the crucial need for in-home robots to utilize the methods of continual learning. In addition to the core continual learning goals highlighted in our examples – mitigating *catastrophic forgetting* (McCloskey & Cohen, 1989; Ratcliff, 1990) and enabling *forward transfer* (Lopez-Paz & Ranzato, 2017) – the robotics setting introduces several distinct challenges.

Robotics is a challenging field for even a single task, as collecting data is time-intensive, supervision is costly (Pari et al., 2021), and significant randomness can cause undesirable damage to both the home and the robot. Additionally, large amounts of resetting would be a burden in a home setting (Zhu et al., 2020a; Eysenbach et al., 2017). Finally, the ability to generalize is critical since real-world settings are never exactly the same; sensor noise, error in robot control, shifts in lighting, and more all result in variation, even in otherwise static scenes. As a result, learning on a real robot for a large enough set of tasks to validate new continuous learning methods has been out of reach. Existing work in the continual learning setting for robotics is limited and largely speculative (Lesort et al., 2020).

To resolve these issues, we propose SANER [1], an adaptation of the SANE algorithm (Powers et al., 2022a) for the robotics imitation setting, which can be used to learn an ensemble of new skills given a handful of unstructured demonstrations of different tasks. To be sufficiently general for robotics, SANER must use a policy that is sample-efficient and robust to noise. Additionally, SANER introduces several significant modifications to enable learning from imitation.

The policy we introduce with SANER is a simple, highly sample-efficient point-cloud-based policy network we call Attention-Based Interaction Policies (ABIP). ABIP is based on PointNet++ (Qi et al., 2017), and was designed to efficiently learn via imitation. ABIP takes inspiration from prior work on perceptually-grounded action spaces for robots (Zeng et al., 2018; 2021; James et al., 2022; Shridhar et al., 2022b; Mo et al., 2021; Wu et al., 2021), which has shown better data efficiency and robustness than directly learning to predict motor commands. Using ABIP, our agents are capable of acquiring new skills with only two demonstrations, minimizing burden on the end-user and robot

---

[1]Code is available at https://github.com/AGI-Labs/continual_rl

Figure 1: On the left we show the entire set of training settings for four tasks: picking and placing a bottle into and out of a sink, and opening and closing an oven. On the right are our evaluation settings. We show how continuous learning techniques like CLEAR (Rolnick et al., 2018) and SANE (Powers et al., 2022a) can be extended to a low-data, learning-from-demonstration setting on a real robot, and can succeed on tasks that vary considerably from the original demonstrations.

alike. While we present ABIP as part of SANER, we believe that its sample efficiency and generalization capacity make it a useful component of any continual learning system for use with robotics.

We evaluate SANER on four kitchen tasks using a low-cost mobile robot: two pick-and-place tasks and two tasks manipulating an articulated object. We demonstrate our method's ability to generalize to unseen object locations, unseen object types, and to clutter, all with very little data. We compare our new method to two other continual learning methods, modified to use ABIP: CLEAR (Rolnick et al., 2018) and EWC (Kirkpatrick et al., 2016). We demonstrate that SANER is more effective at both learning without forgetting and forward transfer in the robotics domain, and that ABIP is a useful component for learning general interaction policies from a small number of examples.

To summarize, in this paper we show for the first time how to modify existing state-of-the-art continual learning methods to a few-shot, real robot imitation learning domain, and describe the necessary algorithmic changes and evaluations. We also describe the requirements on a policy architecture which will make these experiments feasible, and provide a first version of such an architecture in ABIP.

2   RELATED WORK

Relevant prior work spans several fields, including continual learning (Parisi et al., 2019), robotics, and imitation learning. We look both at prior work in continuous learning, reinforcement learning, and in learning generalizable robot policies.

Continual learning for robotics. Continual learning began as the study and mitigation of catastrophic forgetting (Mc-Closkey & Cohen, 1989; Ratcliff, 1990; Robins, 1995). It has since expanded to include forward transfer (Lopez-Paz & Ranzato, 2017) and maintaining plasticity (Mermillod et al., 2013), and more recently, generalization and sample efficiency (Powers et al., 2022b). In this work, we focus on generalization and sample efficiency in the context of visuomotor policy learning, in addition to forgetting, as these are critical pieces for robotics.

While a significant amount of work has focused on continual learning for supervised image classification (Lange et al., 2019), this too has expanded with time to include unsupervised learning (Bagus et al., 2022) and reinforcement learning (Kirkpatrick et al., 2016). Continual learning in robotics has received some attention (Lesort et al., 2020), but while there have been a few works in simulation (Wolczyk et al., 2021; Zentner et al., 2021; Gaya et al., 2022), little has been put into practice. Key exceptions include work by Rusu et al. (2017), which uses Progressive Networks (Rusu et al., 2016) to apply continual learning to the sim2real problem; Gao et al. (2021) utilize deep generative replay for the domain of continual imitation learning for robotics, using 15 demonstrations per real-world task, but their method requires using generative models to create whole new datasets in the new environment in order to avoid forgetting. Chen et al. (2022) propose an approach which constructs policy mixtures for continuous control tasks, but can't learn visuomotor policies or generalize to different scenes.

One other route to continual learning for robotics would be, instead of learning visuomotor skills, to focus on grasp estimation and planning. In general, this sort of pipelined approach is brittle, failing due to occlusions or interference (Kase et al., 2020), and existing open-set grasp estimation methods do not do task-oriented grasping (Newbury
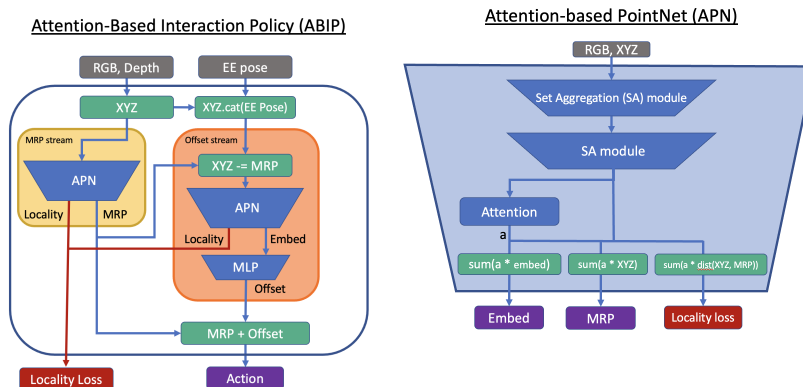
2

Figure 2: Attention-based interaction policies (ABIP). We build an architecture which ignores variations and distractors by first predicting a *Most Relevant Point* (MRP), and then predicting an offset from this point. ABIP is trained with a *locality loss* which penalizes attending to points far from the robot's current position.

et al., 2022). Lomonaco & Maltoni (2017) proposed a continuous object detection dataset, which could have some overlap for our methods, but uses only RGB data, which is far less useful for robust grasping (Newbury et al., 2022). Others have used continuous learning for object detection on real robots (Ayub & Wagner, 2020; Ayub & Fendley, 2022), but have not looked into reactive skill learning. However, ideas from continuous learning for object detection could be used in conjunction with SANER in the future to improve semantic learning and generalization.

Modular RL for robotics. SANE, on which SANER is based, is an ensemble method based on the idea that having separate modules side-steps the problem of catastrophic forgetting. The idea of re-usable robotic skill libraries from demonstrations has been seen in Tanneberg et al. (2021); Behbahani et al. (2021); Peng et al. (2019); Devin et al. (2016), amongst many others (Zentner et al., 2021). Additionally, there has been work to apply modular methods to the continual robotics domain, such as in Mendez et al. (2022), which looks at modular reinforcement learning in the simulated RoboSuite Zhu et al. (2020b) environment, and Ben-Iwhiwhu et al. (2022), which looks at lifelong reinforcement learning in a variety of simulated environments. These are relevant but not directly comparable to our work because much more data is available to train policies in these settings. Others have noted zero-shot generalization as an important problem for RL, for example Kirk et al. (2023) looks at avoiding overfitting to training environments through various means. In our case, we avoid overfitting through a mixture of augmentation and design of an attention-based, perception-driven robot policy.

Perception-driven robot learning. Recent work in robot learning focuses on building general, multi-purpose policies which can scale to a variety of scenarios based on sensor data. Much of this work has likewise focused on big-data settings. In Say-Can (Ahn et al., 2022) and RT-1 (Brohan et al., 2022), for example, the authors use a large dataset to train a multi-task, language-conditioned transformer model. Given that these works require large amounts of data to train, they are not necessarily suitable for online teaching of robot skills in a home environment.

Conversely, there is a thread of work which functions on much smaller amounts of data but still achieves strong performance (Zeng et al., 2018; 2021; Hundt et al., 2020; James et al., 2022; Shridhar et al., 2022a;b). These works focus on a perceptual action space, where actions taken directly correlate with visual features, but often focus on a 2D vision of the world as a result (Zeng et al., 2018; Hundt et al., 2020; Zeng et al., 2021; Shridhar et al., 2022a).

Recent work extended this sort of approach to deal with 3D environments more suitable for robotics tasks (Shridhar et al., 2022b), but still uses very large transformer models that take a long time to train. An alternative is proposed by work like Where2Act (Mo et al., 2021) and VAT-Mart (Wu et al., 2021), which learn a point-cloud based policy which predicts an *interaction point* and a corresponding trajectory. These are based on the powerful Pointnet++ (Qi et al., 2017) backbone, which provides convolutional-equivalent operators that work in 3d space. However, these policies are *open-loop*, meaning that they cannot recover from failures. We build off this work, using a similar representation but modified to be slightly more general.

3 METHOD

We envision a home robot that learns an ever-growing library of skills. These skills could then be expanded, built upon, re-used, and perhaps even shared between agents in the future. To achieve this, we propose SANER, an adaptation of SANE (Powers et al., 2022a) for Robotics.

SANE is an algorithm for the automatic creation and re-use of skill modules; we provide an overview in Section 3. To be suitable in the imitation learning setting, SANER makes several key changes. We break the necessary modifications up as follows: first, we discuss the new policy architecture used by each module, *Attention-Based Interaction Policies* (ABIP), in Section 3.2; second, we discuss changes to the critic in Section 3.3; and third, we discuss changes to module creation in Section 3.4. Additionally, we modify two other continual learning methods, CLEAR and EWC, to use ABIP as well. We describe these adaptations in Section 3.5.

3.1 PRELIMINARIES

Problem Statement Formally, we define an experiment as an ordered sequence of N tasks, $(\mathcal{T}_0...\mathcal{T}_{N-1})$. During training, each task is specified by k_{demo} demonstrations, where each demonstration is given as a trajectory of state, action pairs: $(\langle s, a \rangle)$. To allow us to assume the Markov property, we additionally augment s with context c, taken as the state of the environment at the beginning of the episode. Each task is trained for T timesteps, using points randomly sampled from the demonstration trajectories. Evaluation is performed by executing our learned policy on the real robot, in k_{unseen} settings. More details on evaluation, including metric definitions, are provided in Section 4.1.

For the experiments presented in this paper, the state is composed of an RGB-D image and the robot joint state, and the action is specified as the position and orientation (as a quaternion) of the end effector in world coordinates, plus the state of the gripper as a continuous variable in the range (-0.2, 0.2). Additionally, we include the fraction of the task completed in the action, which is used to determine the end of the episode. We use $N = 4$, $k_{demo} = 2$, k_{unseen}, and $T = 10000$.

Overview of SANE SANE is a task-id-free method that automatically detects and responds to drift in the setting by maintaining an *ensemble* of models called *nodes*. It does this by activating, merging, and creating modules automatically as follows: (1) Each module in its ensemble computes an activation score using a neural network we call the *critic*; for a particular context, the node with the highest score is the one used. (2) As the node improves at the task, a stored version of the critic called the *anchor* is updated. (3) A new node is created when the predicted activation score falls below the value predicted by the anchor by an amount that exceeds some allowed tolerance. This tolerance is called the *uncertainty*, and is also predicted by the critic.

It is important to note that SANE uses CLEAR for each of its modules. CLEAR is a replay buffer method that uses reservoir sampling to give each sample an equal probability of remaining in the buffer, regardless of when it was collected. In the context of SANE, this helps the critic maintain a more accurate representation of the policy's capabilities. Since optimally a single task will activate a single SANE module, we use CLEAR for evaluate ABIP performance and single-task performance.

3.2 ATTENTION-BASED INTERACTION POLICY (ABIP)

Intuitively, in a cluttered and constantly changing setting like a human home, there will be many irrelevant details in the background of any demonstration that a user provides to SANER. Therefore, we split the action prediction problem into two steps: (1) we predict a *Most Relevant Point*, or MRP, which tells us which region of the world the policy must attend to; and (2) we reactively predict *actions* which determine where the robot should move in relation to that MRP: for example, how to approach the handle of an oven and when to close the gripper to grasp it.

These two operations are performed sequentially using a modified PointNet++ (Qi et al., 2017) model that we refer to as *Attention-based PointNet* (A-PointNet), shown in Figure 2. The *MRP Predictor* can then be agnostic to the position of the robot, instead focusing on the features of the object relevant to the overall task, while the *Action Predictor* can learn to focus on features relevant just to what the next action should be. For example, in Figure 7, the MRP Predictor learns to focus on the handle; the Action Predictor focuses on the angle of the oven door.

Image Pre-Processing First we convert the RGB and depth images into a point cloud. We augment the point cloud of the current timestep with our context c, the point cloud from the beginning of the episode. This aids both in combating occlusion, as well as in disambiguating between similar observations that occur during different trajectories. To reduce compute, we crop the working area to 1m, and down-sample using grid pooling, with a resolution of 1cm for the current timestep and 2.5cm for the context. Specifically, we select a random point in each voxel, to reduce overfitting.

3.2.1 ATTENTION-BASED POINTNET (A-POINTNET)

Our Attention-Based PointNet module (A-PointNet), a core component of both our MRP and Action Prediction streams, augments PointNet++ via the addition of an attention mechanism, allowing us to learn to ignore irrelevant details of the scene.

In more detail, A-PointNet passes the point cloud through two set aggregation modules that process information at different scales, as in PointNet++ (Qi et al., 2017). This allows us to harness both structural information from the scene as well as the finer details necessary for manipulation. Further detail on these networks is provided in Appendix 7.7.

The output from the second set aggregation module (Qi et al., 2017) is a reduced point cloud P. We concatenate the embedding, m_i, and position, p_i, of each point i and pass these into an attention network, which is an MLP with output dimension 1, and softmax the resulting values to compute the attention value, a_i. This attention is then used to produce both a weighted average position, $\bar{p} = \sum_{i \in P} a_i p_i$ and a weighted average embedding, $\bar{m} = \sum_{i \in P} a_i m_i$.

This version of attention can be seen as analogous to the spatial attention maps used by CBAM (Woo et al., 2018), using set aggregation modules in place of convolution. The context of each point, which determines its importance, is determined by the structure of points in its neighborhood. For example, the oven is present in every task; however, as we can see in Figure 7, it is attended to less in the presence of a bottle, since a different task is being implicitly indicated in our aggregated embeddings.

3.2.2 Dual-Stream Architecture

Most Relevant Point (MRP) Prediction. Ideally, finding the most relevant point for a particular task would allow us to focus only on high-level task relevant information, ignoring background objects and distractors. To encourage this, we remove points from the point cloud in a rectangular prism surrounding the known location of the end-effector. Due to the fact that when using only a small number of demonstrations the current position of the end-effector is a highly accurate signal for the next position; as discussed in Sec. 4.3, an MRP predictor without this augmentation tends to overfit to these points. This point cloud is then passed into an A-PointNet module to compute a weighted average position, our Most Relevant Point (MRP).

Action Prediction. We then predict actions relative to the MRP. In this case the position of the end-effector is highly relevant to the computation of the next desired action. Therefore, we again remove the points around the end-effector, but now we add a rectangular prism in the position and orientation of the end-effector. This is because the end-effector is often occluded, and here we want to ensure it's available for use.

As before, this point cloud is then passed into a separate A-PointNet module. The resulting $\bar{p}$ and $\bar{m}$ are concatenated, along with the current state of the gripper, then passed into four separate MLPs, which compute the position offset (Δp), rotation (as a quaternion), and gripper state of the end-effector, as well as a prediction for the fraction of the task completed. The offset is added to the MRP to compute the final end-effector position.

3.2.3 Training ABIP

Imitation Loss. To train the policy, we use the action from the demonstration to supervise the position, gripper state, and completion fraction using a mean-squared error loss. We represent orientation as a quaternion and use $1 - (q_{true} \cdot q_{pred})^2$ as the loss, based on Huynh (2009).

Offset Loss. We additionally compute a loss that drives the computed offset toward 0, to further encourage the MRP to encode information relevant to the interaction: $L_{offset} = ||\bar{p}_{off}||_2$

Locality Loss. We encourage generalization with a *locality loss* which encourages relevant points to be close together, defined in Equation 1:

$$L_{local} = \sum_{i \in P} a_i ||p_i, \bar{p}_i||_2 \tag{1}$$

Since these points must also contain information relevant to the task, this allows for a natural convergence of attention around a salient point in the observed point cloud. In effect, this allows us to more quickly learn to ignore irrelevant features of the environment, such as walls or the table surface, allowing for improved generalization.

Removal of Cloning Losses While SANE uses the policy and value cloning losses from CLEAR, which help maintain old behavior in the presence of new data, with SANER this is unnecessary, as we are already training on the true actions observed from the demonstrations.

Removal of Policy Augmentation Unlike in SANE, SANER trains the policy only on new data (B_{new}), not a batch augmented from the replay buffer (B_{aug}). This allows the module to specialize the new policy to the new setting as quickly as possible. This is related to policy freezing, discussed in Section 3.4.

3.3 CRITIC

SANE uses a reinforcement learning critic to estimate two values, a score and an uncertainty, that are used to determine which module to activate and to detect when drift has occurred. For SANER, both of these need to be changed to work in the imitation learning setting.

Critic Architecture In addition to the ABIP policy network, SANER uses a separate A-PointNet encoder for the critic, plus a 3 layer MLP with hidden dimension 64 to predict the value and uncertainty. Unlike in SANE, SANER does not share weights between the actor and the critic. Note that the critic does not utilize a locality loss; we found that earlier tasks might focus too strongly on features that were insufficient signals for future tasks, and the critic's performance would suffer.

Activation Score Conceptually, the goal of SANE's activation score is to evaluate how well each module will perform in the current context. When applied to the reinforcement learning setting, the standard critic is a natural choice, as it is already designed for that purpose. However, in the imitation learning setting, the choice is less clear.

An activation score should: (1) always be greater than 0, to minimize unnecessary module creation at the beginning of training; (2) have a consistent maximum value, for consistency between tasks and to make hyperparameter selection easier – we choose a maximum of about 3; and (3) be highly sensitive to policy errors on about the same scale as the hardware and tasks permit, and less sensitive to the difference between large errors in action prediction.

Our last criteria is both the most important and the least trivial. Say we have a module that succeeds at a particular task with an error in the predicted-end effector position of about 1cm. If updates to the policy that induce an error of 2cm would cause the module to start failing at the task, then the score function should drop considerably. However for the same task, if a different module has a policy error of, say, 18cm, then an increase to 20cm should have little effect on the score; both are clear failures, and should be near 0.

While there are a number of options for functions that meet this criteria, we found it most straightforward to compute a target score based on the distance between the true action and the predicted action. Specifically, we use: $s_{target} = softplus(\beta)(a||p_{true}, p_{pred}||_2) + b$, where p_{true} is the true end-effector position, p_{pred} is the current prediction of the policy, and a, b, and β are constants. We use essentially this same metric for the orientation and gripper pose as well, and sum the results to achieve our final score. More details on the selection of these constants is described in Appendix 7.10. We then train the critic to predict this target score using an L1 loss.

Uncertainty Estimation In imitation learning, the policy learns much more quickly than in reinforcement learning, due to the fact that RL relies upon credit assignment instead of direct supervision, causing learning to take orders of magnitude more time. While faster training is generally beneficial, we found that our prediction of uncertainty tended to lag behind the performance of the policy, particularly at the beginning of a task when the policy is changing rapidly. To resolve this, we introduce a multiplicative factor on the uncertainty, for both the new node and the source node, that increases when drift is detected, and decays as the module is used. This gives the uncertainty estimator more time to converge accurately.

More specifically, we defined our modified uncertainty as $u' = (1+f) * u$, where u is the standard uncertainty predicted by SANE, and f is our uncertainty factor. When a drift event is detected and a node is created, f is incremented by k_s for the source node and k_n for the new node. When a node is activated, its f decays according to: $f_{t+n} = f_t * \gamma^n$, where n is the number of timesteps seen by the module during activation.

In SANE, uncertainty is used for node activation and upper bound estimation. We can therefore define f_{act} and f_{ub} separately, with separate k and γ values for each. This is useful because, for example, while we want the source node's uncertainty to be reflected in its upper bound to mitigate unnecessary node creation, we do not need the source node to be more likely activate. Uncertainty is also used for lower bound estimation; however, a sensitive lower bound poses little issue, and we therefore neglect f for this case.

Replay augmentation. In reinforcement learning it is not feasible to mine negative examples for one module from the others, because it is challenging to estimate what outcome a policy will have in an environment without actually doing it. However, with imitation learning, mining negative examples is trivial. We leverage this advantage by, at each activation step, giving the active module a 10% chance to exchange a few samples with each other module.

Handling noisy predictions. While ABIP is training, the point cloud augmentations, particularly the random downsampling before the first set aggregation module, can result in critic predictions with significant noise. We found that the slow critic SANE uses to smooth training did little to impact this source of noise. We opt to remove the slow critic, and instead average all critic computations over 5 runs of the same observation.

3.4 MODULE CREATION

The main way that catastrophic forgetting is mitigated in SANE is by the creation of new modules (Powers et al., 2022a), which allows one to persist prior behavior, while the other learns the new task. Creation occurs when an active module's critic predicts an upper bound on predicted value that is lower than the prediction of its anchor. With imitation learning however, once that has happened, the policy has already changed considerably, and significant forgetting has already occurred.

We mitigate this issue in SANER with a naïve strategy: once a module is cloned, we reset both the policy and the critic to their states at the last time the anchor was updated, which is effectively our last known good state. Furthermore, we freeze the policy, preventing it from training further.

3.5 ADAPTING EXISTING BASELINES

Existing continual-learning methods require a few changes to be applied to the learning-from-demonstration context we want to use for our home robotics setting. In particular, we adapted CLEAR and EWC using same change in loss made for SANER: using the changes to the loss from Section 3.2.3 in place of V-trace, with the exception that we do not remove policy augmentation for CLEAR, and it is not applicable for EWC.

4 EXPERIMENTAL SETUP

We demonstrate continual learning in robotics in a kitchen environment by doing the following 4 tasks: picking up a bottle and putting it in the sink, taking a bottle out of the sink, opening a toaster oven, and closing a toaster oven. For each task we collected and train on only two demonstrations.

We perform three evaluations: first, we demonstrate the generalization ability of ABIP on each task independently, second we ablate our key novel contributions on ABIP, and finally we evaluate our continual learning methods on the tasks trained in sequence.

Robotic platform. We utilize the Hello Robot Stretch[2] (Kemp et al., 2021) in all our experiments, shown in Figure 1. The Stretch robot is a "low cost" robot, composed of an arm that can independently move vertically and horizontally, a wrist with 3 rotational degrees of freedom, and a pinching gripper. The base is also capable of motion, but for our experiments we keep the robot stationary, leaving this for future work. The camera used to collect observation data is a RealSense D435 mounted on the head of the robot, and remained stationary during all episodes. Demonstration collection, training, and inference were done off-robot on a dedicated desktop, and communication with the robot was done via ROS.

Task selection. The tasks were chosen to highlight a variety of kitchen-relevant sub-skills, under the constraint that there are 5 degrees of freedom in the motion of the arm. The two primary skills exercised are pick-and-place and manipulation of an articulated object. The entirety of our train and test settings can be seen in Figure 1, where the opening and closing of the oven are two tasks using the same settings. Notice that with only small perturbations of the object of interest, we observe significant ability to generalize.

Specifically, picking the bottle from the sink requires a precise approach, as pushing the bottle is risky and may tip the bottle. During our evaluations, we move the bottle in all three dimensions, to evaluate the agent's ability to generalize accurately. The choice of a bottle partially filled with water is convenient, as it allows for tuning the task's sensitivity to imprecise actions. Picking the bottle from the counter is easier in both these respects, allowing us to use this setting to test more significant displacements in all dimensions, as well as robustness to clutter.

The toaster oven, by contrast, requires learning the curved trajectory of a closing door. An agent that cannot execute the oven interactions accurately will often get stuck, and will need to retreat and re-grasp, as for example is shown in the Appendix in Figure 6. We train on two different ovens, and demonstrate generalization using an unseen oven in differing positions, and in the presence of clutter.

Beyond evaluating these specific sub-skills, the tasks we have chosen provide an efficient test-bed for continual learning specifically: multiple interactions with the same object provides opportunity for forward transfer, while similar observations with conflicting behaviors is an efficient way to elicit catastrophic forgetting.

We collected two demonstrations for each task, and execute 3 out-of-distribution trials. While training the agent on a task, we sample transitions randomly from both demonstrations. More information can be found in Appendix 7.9.

---

[2]hello-robot.com/

Collecting demonstrations. We guided the robot through the trajectory using a controller, recording actions at critical points (key points) as in prior work (Shridhar et al., 2022b). At each key point, we collect the RGB and depth images, as well as the robot's joint states. The joint states are converted into end-effector position and orientation using forward kinematics. More detail and an example demonstration are shown in Appendix 7.2.

Implementation Details SANER is based on an implementation of SANE utilizing IMPALA (Espeholt et al., 2018), as provided by CORA (Powers et al., 2022b). Each module has a replay buffer size of 625. Since four modules were created during training, SANER uses a total number of 2500 stored frames. CLEAR and EWC were also implemented using IMPALA. For consistency we set CLEAR's total number of replay frames to be 2500. All other hyperparameters are given in Appendix 7.7.2.

EWC Unfortunately, while we tried training EWC using λ in [1000, 10000, 100000], we found no value that worked reasonably in our setting, and opted not to run EWC on the robot. More detail is provided in Appendix 7.

4.1 EVALUATION

Evaluation was run by randomly selecting one of the two demonstrations, and initializing the robot to its starting configuration. We scored performance according to a rubric, with partial task completion earning partial credit. Scoring details are given in Appendix 7.9. Roughly speaking, the robot earns a higher reward the more of the trajectory it successfully executes.

For ABIP performance and ablations, we present the mean of reward over three trials. For the continual learning results presented in Section 4.4, we captured performance data before and after training on each task, as well as final performance at the end of each run. While it might be preferred to collect data for *all* tasks at the end of each task, or even significantly more frequently as per Kirkpatrick et al. (2016), this is infeasible due to the time-consuming nature of real-robot experiments. Additionally, we never test in comparison with a randomly-initialized policy as in Chaudhry et al. (2018), to avoid damage to the robot or environment.

Metrics. We use the following metrics, based upon existing methods (Chaudhry et al., 2018; Powers et al., 2022b), modified to capture the most information using the fewest number of interactions with the environment.

We use the notation that $R_{x,y}$ indicates average performance on task x after training on task y, where $y = \oslash$ indicates before training on anything, and N indicates the index of the final task. R_x indicates the average performance on a task trained alone (non-sequentially). We assume the reward of a random policy, $R_{i,\oslash}$, is approximately 0, which will hold in general for complex tasks with a short time horizon. We additionally assume tasks are only seen once, not cyclically.
- Final performance $R_{final,i} = R_{i,N}$: reward after training is completed on all examples.
- Performance improvement $\Delta R_i = R_{i,i} - R_{i,i-1}$: change in reward/score by training on the task.
- Zero-shot forward transfer $ZSFT_i = R_{i,i-1} - R_{i,\oslash} \approx R_{i,i-1}$: reward achieved at the very start of a task, before any explicit training on it is done.
- Cumulative forgetting $F_i = R_{i,i} - R_{i,N}$: decline in reward after learning new skills.
- Intransigence $I_i = R_i - R_{i,i}$: relative inability to learn compared to a stand-alone model

The first four metrics only require that we evaluate a policy's performance on two tasks at each task transition – the task just trained, and the task about to be trained – and on all tasks once at the end. The fifth metric, intransigence, additionally requires that we train and evaluate a separate model per task. This simplification from the standard, of evaluating across all tasks, allows our evaluation to scale linearly in the number of tasks, instead of quadratically.

Zero-shot forward transfer, performance improvement, and cumulative forgetting together provide us with an overall view of the lifetime of performance for each task: ZSFT indicates how much of a direct boost prior tasks provided, ΔR indicates direct improvement from training on the task, and F tells us how much is lost via the remainder of the tasks. Finally, where ZSFT tells us of the immediate impact prior tasks had, intransigence tells us about the latent effects, e.g. via decreased capacity or ineffective representation.

To make at-a-glance comparison easier, we present F and I as $-F$ and $-I$ instead; this is because the rest of the metrics indicate better performance the larger they are, whereas these two, by convention, are worse. We refer to $-F$ as recall, and $-I$ as plasticity.

4.2 EVALUATING ATTENTION-BASED INTERACTION POLICIES

First, we examined the ability of ABIP to generalize to out-of-distribution variations of each task. We trained on each task separately using CLEAR (Rolnick et al., 2018), and then evaluated on each of the training settings, as well as in the out-of-distribution generalization settings visualized in Figure 1. Results are shown in Table 1.

Task	In Distribution: Demo 0	In Distribution: Demo 1	Out of Distribution
Bottle To Sink	0.80 ± 0.34	0.87 ± 0.23	1.0 ± 0.0
Bottle From Sink	0.60 ± 0.40	1.0 ± 0.0	0.47 ± 0.23
Open Oven	0.20 ± 0.20	0.80 ± 0.20	0.87 ± 0.11
Close Oven	0.53 ± 0.50	0.33 ± 0.12	1.0 ± 0.0
Average	0.53	0.75	0.83

Table 1: Performance of CLEAR (Rolnick et al., 2018) on "in distribution" and "out of distribution" tasks, using ABIP as the underlying policy representation. We observe significant generalization ability.

	ABIP	No MRP Locality	No Offset Locality	Single Stream	No MRP
Bottle to Sink	1.0 ± 0.0	0.0 ± 0.0	0.67 ± 0.57	0.0 ± 0.0	0.067 ± 0.12

Table 2: Ablation experiments on the generalization (out-of-distribution) setting. ABIP provides better generalization from very few examples, including robustness to unseen, out-of-distribution object poses and new objects.

Our specific goal is to demonstrate that this model is sufficiently capable of learning skills in the few-shot setting, in order to be useful as a building block of a continual learning system. For this to be the case: (1) ABIP must learn well enough that catastrophic forgetting would be observable, (2) the domain must be challenging enough for forward transfer to be meaningful, and (3) general representations and policies must be attainable, so that the skills learned are practical.

We see generally high performance across both in-distribution and out-of-distribution settings, with a few exceptions. While performance is not directly comparable, we see that our method compares favorably to similar settings presented by other work using the Stretch in the home environment (Bahl et al., 2022; Parashar et al., 2023; Pari et al., 2021) As discussed above, ABIP's performance on each task highlights different strengths and weaknesses of the method. The method performs well on the *Bottle To Sink* task, particularly on the unseen settings, which indicates that the method is robust to significant displacements of the target object, and to distractors – key features of our MRP-based method. It suffers a bit on the *Bottle From Sink* generalization task, however. This task is highly sensitive to small errors in grasp trajectory, which indicates that while the MRP is capable of identifying our object, the action prediction is an area of improvement.

Overall, it is clear that ABIP can capture our task, and that the task is challenging enough to be interesting. Additionally, we specifically demonstrated both that the method is capable of generalizing to objects in unseen, out-of-distribution positions, as well as to unseen objects. Our policies were able to adapt to significant shifts in position and scene composition, including being able to open and close an unseen oven.

4.3 ABIP ABLATIONS

Having demonstrated that ABIP is a capable building block for continual learning, we proceed to analyze the effects of the design decisions made in its creation. In particular, we ablate by comparing the ABIP to methods that: 1) remove the locality loss for the MRP, 2) remove the locality loss for the offset, 3) use a single-stream variant of the model where the MRP is predicted in the same stream as the offset, 4) use a version with no MRP at all. Results are shown in Table 2. All results are provided as the average over three generalization trials.

ABIP outperforms the ablations significantly, with three of the four failing to achieve anything better than a partial grasp. When trained without the locality loss on the offset-prediction head, by contrast, the model succeeded in completing two full trajectories, but failed entirely at the third. However, the case where it failed is informative: it was the setting with distractor objects.

In summary, ABIP has qualitatively better representations for generalization, finds the object of interest more reliably, and is more capable of executing trajectories to completion.

4.4 SEQUENTIAL TASKS

We compared the performance of SANER and CLEAR in our continual learning setting, where we train sequentially on 4 tasks. We evaluate only on the generalization settings; results are given in Table 3. While CLEAR tends to learn more via direct task training (ΔR), it also exhibited significant forgetting, particularly on the bottle tasks By contrast,

Figure 3: Visualization of the attention for the MRP for SANER as it evolves over the episode, showing convergence to the object of interest. The MRP is represented, where visible, with a blue sphere.

| | Single Task | CLEAR | | | | | SANER | | | | |
	R_i	R_{final}	ΔR	ZSFT	-F	-I	R_{final}	ΔR	ZSFT	-F	-I
Bottle To Sink	1.0	0.067	0.87	—	-0.80	-0.13	0.33	0.33	—	0	-0.67
Bottle From Sink	0.47	0.13	0.067	0.20	-0.13	-0.33	0.13	-0.067	0.13	0.067	-0.40
Open Oven	0.87	0.33	0.20	0.0	0.13	-0.60	0.33	0.33	0.0	0.0	-0.53
Close Oven	1.0	0.87	0.73	0.13	0.0	0.13	0.87	0.20	0.67	0.0	-0.13
Average	0.84	0.35	**0.47**	0.11	-0.20	**-0.30**	**0.42**	0.20	**0.26**	**0.017**	-0.44

Table 3: Comparison of two methods for continual learning: CLEAR and SANER, as demonstrated on our setting given only a handful of demonstrations, across a number of different metrics. We have negated Forgetting (F) and Intransigence (I) so that in all cases a larger number is preferred.

SANER uniformly maintains what it has learned, even exhibiting increased performance on the "Open Oven" task after training on later tasks.

Additionally, whereas CLEAR observed *some* zero-shot forward transfer, SANER experienced a considerable amount, on the "Close Oven" task in particular. This likely contributes to SANER's lower ΔR score, as it was largely capable of solving the task prior to training on it. Due to SANER's ensemble nature, it is likely that the separation of representations enabled a more seamless transfer than was possible with CLEAR's single network.

Qualitatively, CLEAR's behavior was somewhat erratic, tending to first approach every object as if it were an oven. In one instance, it executed a seamless oven opening trajectory against the side of a toaster, and in another it grabbed the handle of the bottle and pulled it down in a similar way. SANER's behavior, while imperfect, is more consistent and interpretable. Since SANER modularizes its behaviors, one can roughly know what SANER will do by observing which module it activated. However, the generally lower performance as compared to the single task setting indicates significant room for improvement. We show an example failure in Fig. 3. Its attention shifts first to the edge of the sink, then to the bottle itself as it attempts a grasp. The grasp, however, fails, due to inaccurate timing of gripper closure. Similar grasp-timing related issues were seen in many of the failures in other tasks as well.

The issue may come down to the fact that CLEAR trains on effectively seven times as much data as SANER. SANER only trains the active module's actor on the current batch of data, instead of an augmented batch, as SANER's critics and CLEAR both do. As such, we see that after training the first task, SANER's loss is twice CLEAR's, giving further support to this hypothesis. We will investigate solutions in future work. Overall, however, SANER has demonstrated utility in the robotics setting, by being able to learn general behavior from only two examples, with essentially no forgetting and a non-trivial amount of forward transfer.

5 CONCLUSIONS

In order to enable robots to operate in the home setting, they need to be able to learn continually from small amounts of data. To this end, we proposed SANER, an ensemble method adapted to the robotics setting. We demonstrated, on a set of 4 kitchen skills, utilizing a Stretch robot, that it is capable of learning new skills and generalizing to unseen settings with forward transfer and while mitigating the effects of catastrophic forgetting, out-performing a strong baseline on these metrics. SANER is built on top of ABIP, which can function as a simple building block capable of learning highly useful, very generalizable interaction policies. Finally, we presented the fundamentals of our environment design and a set of continual learning metrics simplified to be viable for the robotics case. In conclusion, we demonstrate how we can deploy continuous learning techniques like SANE (Powers et al., 2022a) and CLEAR (Rolnick et al., 2018) to a limited-data robotics context.

6 ACKNOWLEDGEMENTS

REFERENCES

Michael Ahn, Anthony Brohan, Noah Brown, Yevgen Chebotar, Omar Cortes, Byron David, Chelsea Finn, Keerthana Gopalakrishnan, Karol Hausman, Alex Herzog, et al. Do as i can, not as i say: Grounding language in robotic affordances. *arXiv preprint arXiv:2204.01691*, 2022.

Ali Ayub and Carter Fendley. Few-shot continual active learning by a robot. *arXiv preprint arXiv:2210.04137*, 2022.

Ali Ayub and Alan R Wagner. Tell me what this is: Few-shot incremental object learning by a robot. In *2020 IEEE/RSJ International Conference on Intelligent Robots and Systems (IROS)*, pp. 8344–8350. IEEE, 2020.

Benedikt Bagus, Alexander Gepperth, and Timothée Lesort. Beyond supervised continual learning: a review, 2022. URL https://arxiv.org/abs/2208.14307.

Shikhar Bahl, Abhinav Gupta, and Deepak Pathak. Human-to-robot imitation in the wild, 2022.

Sanaz Behbahani, Siddharth R. Chhatpar, Said Zahrai, Vishakh Duggal, and Mohak Sukhwani. Episodic memory model for learning robotic manipulation tasks. *CoRR*, abs/2104.10218, 2021. URL https://arxiv.org/abs/2104.10218.

Eseoghene Ben-Iwhiwhu, Saptarshi Nath, Praveen K. Pilly, Soheil Kolouri, and Andrea Soltoggio. Lifelong reinforcement learning with modulating masks, 2022. URL https://arxiv.org/abs/2212.11110.

Anthony Brohan, Noah Brown, Justice Carbajal, Yevgen Chebotar, Joseph Dabis, Chelsea Finn, Keerthana Gopalakrishnan, Karol Hausman, Alex Herzog, Jasmine Hsu, et al. Rt-1: Robotics transformer for real-world control at scale. *arXiv preprint arXiv:2212.06817*, 2022.

Arslan Chaudhry, Puneet Kumar Dokania, Thalaiyasingam Ajanthan, and Philip H. S. Torr. Riemannian walk for incremental learning: Understanding forgetting and intransigence. *CoRR*, abs/1801.10112, 2018. URL http://arxiv.org/abs/1801.10112.

Letian Chen, Sravan Jayanthi, Rohan Paleja, Daniel Martin, Viacheslav Zakharov, and Matthew Gombolay. Scalable lifelong learning from heterogeneous demonstrations. *IROS Workshop on Lifelong Robot Learning*, 2022.

Coline Devin, Abhishek Gupta, Trevor Darrell, Pieter Abbeel, and Sergey Levine. Learning modular neural network policies for multi-task and multi-robot transfer. *CoRR*, abs/1609.07088, 2016. URL http://arxiv.org/abs/1609.07088.

Lasse Espeholt, Hubert Soyer, Rémi Munos, Karen Simonyan, Volodymyr Mnih, Tom Ward, Yotam Doron, Vlad Firoiu, Tim Harley, Iain Dunning, Shane Legg, and Koray Kavukcuoglu. IMPALA: scalable distributed deep-rl with importance weighted actor-learner architectures. *CoRR*, abs/1802.01561, 2018. URL http://arxiv.org/abs/1802.01561.

Benjamin Eysenbach, Shixiang Gu, Julian Ibarz, and Sergey Levine. Leave no trace: Learning to reset for safe and autonomous reinforcement learning. *CoRR*, abs/1711.06782, 2017. URL http://arxiv.org/abs/1711.06782.

Chongkai Gao, Haichuan Gao, Shangqi Guo, Tianren Zhang, and Feng Chen. CRIL: continual robot imitation learning via generative and prediction model. *CoRR*, abs/2106.09422, 2021. URL https://arxiv.org/abs/2106.09422.

Jean-Baptiste Gaya, Thang Doan, Lucas Caccia, Laure Soulier, Ludovic Denoyer, and Roberta Raileanu. Building a subspace of policies for scalable continual learning, 2022. URL https://arxiv.org/abs/2211.10445.

Andrew Hundt, Benjamin Killeen, Nicholas Greene, Hongtao Wu, Heeyeon Kwon, Chris Paxton, and Gregory D Hager. "good robot!": Efficient reinforcement learning for multi-step visual tasks with sim to real transfer. *IEEE Robotics and Automation Letters*, 5(4):6724–6731, 2020.

Du Q. Huynh. Metrics for 3d rotations: Comparison and analysis. *Journal of Mathematical Imaging and Vision*, 35: 155–164, 2009.

Stephen James, Kentaro Wada, Tristan Laidlow, and Andrew J Davison. Coarse-to-fine q-attention: Efficient learning for visual robotic manipulation via discretisation. In *Proceedings of the IEEE/CVF Conference on Computer Vision and Pattern Recognition*, pp. 13739–13748, 2022.

Kei Kase, Chris Paxton, Hammad Mazhar, Tetsuya Ogata, and Dieter Fox. Transferable task execution from pixels through deep planning domain learning. In *2020 IEEE International Conference on Robotics and Automation (ICRA)*, pp. 10459–10465. IEEE, 2020.

Charles C. Kemp, Aaron Edsinger, Henry M. Clever, and Blaine Matulevich. The design of stretch: A compact, lightweight mobile manipulator for indoor human environments. *CoRR*, abs/2109.10892, 2021. URL https://arxiv.org/abs/2109.10892.

Robert Kirk, Amy Zhang, Edward Grefenstette, and Tim Rocktäschel. A survey of zero-shot generalisation in deep reinforcement learning. *Journal of Artificial Intelligence Research*, 76:201–264, 2023.

James Kirkpatrick, Razvan Pascanu, Neil C. Rabinowitz, Joel Veness, Guillaume Desjardins, Andrei A. Rusu, Kieran Milan, John Quan, Tiago Ramalho, Agnieszka Grabska-Barwinska, Demis Hassabis, Claudia Clopath, Dharshan Kumaran, and Raia Hadsell. Overcoming catastrophic forgetting in neural networks. *CoRR*, abs/1612.00796, 2016. URL http://arxiv.org/abs/1612.00796.

Matthias De Lange, Rahaf Aljundi, Marc Masana, Sarah Parisot, Xu Jia, Ales Leonardis, Gregory G. Slabaugh, and Tinne Tuytelaars. Continual learning: A comparative study on how to defy forgetting in classification tasks. *CoRR*, abs/1909.08383, 2019. URL http://arxiv.org/abs/1909.08383.

Timothée Lesort, Vincenzo Lomonaco, Andrei Stoian, Davide Maltoni, David Filliat, and Natalia Díaz-Rodríguez. Continual learning for robotics: Definition, framework, learning strategies, opportunities and challenges. *Information fusion*, 58:52–68, 2020.

Vincenzo Lomonaco and Davide Maltoni. Core50: a new dataset and benchmark for continuous object recognition. In *Conference on Robot Learning*, pp. 17–26. PMLR, 2017.

David Lopez-Paz and Marc' Aurelio Ranzato. Gradient episodic memory for continual learning. In I. Guyon, U. Von Luxburg, S. Bengio, H. Wallach, R. Fergus, S. Vishwanathan, and R. Garnett (eds.), *Advances in Neural Information Processing Systems*, volume 30. Curran Associates, Inc., 2017. URL https://proceedings.neurips.cc/paper/2017/file/f87522788a2be2d171666752f97ddebb-Paper.pdf.

Michael McCloskey and Neal J. Cohen. Catastrophic interference in connectionist networks: The sequential learning problem. volume 24 of *Psychology of Learning and Motivation*, pp. 109–165. Academic Press, 1989. doi: https://doi.org/10.1016/S0079-7421(08)60536-8. URL https://www.sciencedirect.com/science/article/pii/S0079742108605368.

Jorge A. Mendez, Harm van Seijen, and Eric Eaton. Modular lifelong reinforcement learning via neural composition, 2022. URL https://arxiv.org/abs/2207.00429.

Martial Mermillod, Aurélia Bugaiska, and Patrick BONIN. The stability-plasticity dilemma: investigating the continuum from catastrophic forgetting to age-limited learning effects. *Frontiers in Psychology*, 4, 2013. ISSN 1664-1078. doi: 10.3389/fpsyg.2013.00504. URL https://www.frontiersin.org/articles/10.3389/fpsyg.2013.00504.

Kaichun Mo, Leonidas J Guibas, Mustafa Mukadam, Abhinav Gupta, and Shubham Tulsiani. Where2act: From pixels to actions for articulated 3d objects. In *Proceedings of the IEEE/CVF International Conference on Computer Vision*, pp. 6813–6823, 2021.

Rhys Newbury, Morris Gu, Lachlan Chumbley, Arsalan Mousavian, Clemens Eppner, Jürgen Leitner, Jeannette Bohg, Antonio Morales, Tamim Asfour, Danica Kragic, et al. Deep learning approaches to grasp synthesis: A review. *arXiv preprint arXiv:2207.02556*, 2022.

Priyam Parashar, Jay Vakil, Sam Powers, and Chris Paxton. Spatial-language attention policies for efficient robot learning, 2023.

Jyothish Pari, Nur Muhammad Shafiullah, Sridhar Pandian Arunachalam, and Lerrel Pinto. The surprising effectiveness of representation learning for visual imitation. *CoRR*, abs/2112.01511, 2021. URL https://arxiv.org/abs/2112.01511.

German I. Parisi, Ronald Kemker, Jose L. Part, Christopher Kanan, and Stefan Wermter. Continual lifelong learning with neural networks: A review. *Neural Networks*, 113:54–71, 2019. ISSN 0893-6080. doi: https://doi.org/10.1016/j.neunet.2019.01.012. URL https://www.sciencedirect.com/science/article/pii/S0893608019300231.

Xue Bin Peng, Michael Chang, Grace Zhang, Pieter Abbeel, and Sergey Levine. MCP: learning composable hierarchical control with multiplicative compositional policies. *CoRR*, abs/1905.09808, 2019. URL http://arxiv.org/abs/1905.09808.

Sam Powers, Eliot Xing, and Abhinav Gupta. Self-activating neural ensembles for continual reinforcement learning. In Sarath Chandar, Razvan Pascanu, and Doina Precup (eds.), *Conference on Lifelong Learning Agents, CoLLAs 2022, 22-24 August 2022, McGill University, Montréal, Québec, Canada*, volume 199 of *Proceedings of Machine Learning Research*, pp. 683–704. PMLR, 2022a. URL https://proceedings.mlr.press/v199/powers22a.html.

Sam Powers, Eliot Xing, Eric Kolve, Roozbeh Mottaghi, and Abhinav Gupta. CORA: benchmarks, baselines, and metrics as a platform for continual reinforcement learning agents. In Sarath Chandar, Razvan Pascanu, and Doina Precup (eds.), *Conference on Lifelong Learning Agents, CoLLAs 2022, 22-24 August 2022, McGill University, Montréal, Québec, Canada*, volume 199 of *Proceedings of Machine Learning Research*, pp. 705–743. PMLR, 2022b. URL https://proceedings.mlr.press/v199/powers22b.html.

Charles Ruizhongtai Qi, Li Yi, Hao Su, and Leonidas J. Guibas. Pointnet++: Deep hierarchical feature learning on point sets in a metric space. *CoRR*, abs/1706.02413, 2017. URL http://arxiv.org/abs/1706.02413.

Roger Ratcliff. Connectionist models of recognition memory: Constraints imposed by learning and forgetting functions. *Psychological Review*, 97(2):285–308, 1990. doi: 10.1037/0033-295x.97.2.285.

Anthony Robins. Catastrophic forgetting, rehearsal and pseudorehearsal. *Connection Science*, 7(2):123–146, 1995. doi: 10.1080/09540099550039318. URL https://doi.org/10.1080/09540099550039318.

David Rolnick, Arun Ahuja, Jonathan Schwarz, Timothy P. Lillicrap, and Greg Wayne. Experience replay for continual learning. *CoRR*, abs/1811.11682, 2018. URL http://arxiv.org/abs/1811.11682.

Andrei A. Rusu, Neil C. Rabinowitz, Guillaume Desjardins, Hubert Soyer, James Kirkpatrick, Koray Kavukcuoglu, Razvan Pascanu, and Raia Hadsell. Progressive neural networks. *CoRR*, abs/1606.04671, 2016. URL http://arxiv.org/abs/1606.04671.

Andrei A. Rusu, Matej Večerík, Thomas Rothörl, Nicolas Heess, Razvan Pascanu, and Raia Hadsell. Sim-to-real robot learning from pixels with progressive nets. In Sergey Levine, Vincent Vanhoucke, and Ken Goldberg (eds.), *Proceedings of the 1st Annual Conference on Robot Learning*, volume 78 of *Proceedings of Machine Learning Research*, pp. 262–270. PMLR, 13–15 Nov 2017. URL https://proceedings.mlr.press/v78/rusu17a.html.

Mohit Shridhar, Lucas Manuelli, and Dieter Fox. Cliport: What and where pathways for robotic manipulation. In *Conference on Robot Learning*, pp. 894–906. PMLR, 2022a.

Mohit Shridhar, Lucas Manuelli, and Dieter Fox. Perceiver-actor: A multi-task transformer for robotic manipulation. *arXiv preprint arXiv:2209.05451*, 2022b.

Daniel Tanneberg, Kai Ploeger, Elmar Rueckert, and Jan Peters. Skid raw: Skill discovery from raw trajectories. *IEEE Robotics and Automation Letters*, 6(3):4696–4703, 2021. doi: 10.1109/LRA.2021.3068891.

Dmitry Ulyanov, Andrea Vedaldi, and Victor S. Lempitsky. Instance normalization: The missing ingredient for fast stylization. *CoRR*, abs/1607.08022, 2016. URL http://arxiv.org/abs/1607.08022.

Maciej Wolczyk, Michal Zajac, Razvan Pascanu, Lukasz Kucinski, and Piotr Milos. Continual world: A robotic benchmark for continual reinforcement learning. *CoRR*, abs/2105.10919, 2021. URL https://arxiv.org/abs/2105.10919.

Sanghyun Woo, Jongchan Park, Joon-Young Lee, and In So Kweon. CBAM: convolutional block attention module. *CoRR*, abs/1807.06521, 2018. URL http://arxiv.org/abs/1807.06521.

Ruihai Wu, Yan Zhao, Kaichun Mo, Zizheng Guo, Yian Wang, Tianhao Wu, Qingnan Fan, Xuelin Chen, Leonidas Guibas, and Hao Dong. Vat-mart: Learning visual action trajectory proposals for manipulating 3d articulated objects. *arXiv preprint arXiv:2106.14440*, 2021.

Andy Zeng, Shuran Song, Stefan Welker, Johnny Lee, Alberto Rodriguez, and Thomas Funkhouser. Learning synergies between pushing and grasping with self-supervised deep reinforcement learning. In *2018 IEEE/RSJ International Conference on Intelligent Robots and Systems (IROS)*, pp. 4238–4245. IEEE, 2018.

Andy Zeng, Pete Florence, Jonathan Tompson, Stefan Welker, Jonathan Chien, Maria Attarian, Travis Armstrong, Ivan Krasin, Dan Duong, Vikas Sindhwani, et al. Transporter networks: Rearranging the visual world for robotic manipulation. In *Conference on Robot Learning*, pp. 726–747. PMLR, 2021.

K. R. Zentner, Ryan Julian, Ujjwal Puri, Yulun Zhang, and Gaurav S. Sukhatme. A simple approach to continual learning by transferring skill parameters. *CoRR*, abs/2110.10255, 2021. URL https://arxiv.org/abs/2110.10255.

Henry Zhu, Justin Yu, Abhishek Gupta, Dhruv Shah, Kristian Hartikainen, Avi Singh, Vikash Kumar, and Sergey Levine. The ingredients of real-world robotic reinforcement learning. *CoRR*, abs/2004.12570, 2020a. URL https://arxiv.org/abs/2004.12570.

Yuke Zhu, Josiah Wong, Ajay Mandlekar, and Roberto Martín-Martín. robosuite: A modular simulation framework and benchmark for robot learning. *arXiv preprint arXiv:2009.12293*, 2020b.

7 APPENDIX

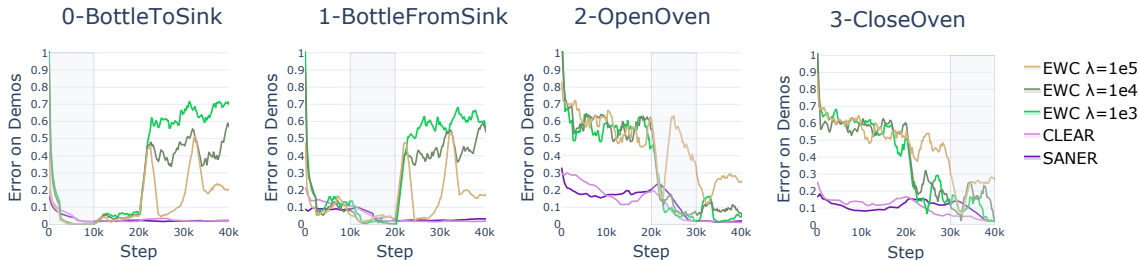### 7.1 EWC COMPARISON: PERFORMANCE ON DEMONSTRATION DATA

Figure 4: Continual evaluation of the error on demonstrations for each of the methods.

Results from evaluating the methods on the demonstration data are shown in Figure 4. The grey box indicates the region where each task was trained. Reported error is the same as the loss used to train the policy.

Note that at the lower λ values for EWC, we observe significant forgetting of the earlier tasks, but at the highest value, latter tasks struggle to learn in the presence of the regularizing EWC loss (triggered after 2k steps of each task). We believe that this indicates that the method is not able to find a single parameter set that is able to solve both tasks. Since error was significant, we opted to not risk damage to the robot or environment by running this policy.

7.2 COMPLEXITY ANALYSIS OF SANER VS CLEAR

Here we analyze the difference in run-time and memory complexity for SANER vs CLEAR.

Space Complexity We hold the total replay buffer size constant for SANER and CLEAR: in the experiments presented in the paper, SANER uses 625 frames for each of 4 modules and CLEAR uses a total of 2500 frames. In longer sets of tasks with more module creation, we would scale as necessary to maintain consistency. Additionally, while we have not found the size of the networks themselves to be a limiting factor, since SANER only activates one module at a time, it would be possible to off-load unused resources as necessary.

Run-time Complexity SANER trains both the actor and the critic for the active module, in contrast to CLEAR which only trains the actor. However, the SANER critic is single-stream (no MRP prediction). In practice, SANER takes a bit less than 2x the time to train as compared to CLEAR.

SANER also runs the critic for every node every 150 time steps during training, to determine which module to activate. There is a trade-off here between activating infrequently (for speed) and how quickly we can detect and react to drift. During evaluation, we run the critic for all nodes, for each episode. Time for activation is the only run-time factor that scales in the number of modules; at the activation and continual evaluation frequencies we selected, however, this is not a dominant factor in the required time to train.

In total, running the 40k timesteps for training these tasks took about 5 hours for CLEAR, and 9.5 hours for SANER.

7.3 DEMONSTRATION DETAILS

Figure 5: The full set of observations for one of the demonstrations for the *Bottle to Sink* task.

Demonstrations were collected using ROS and a dedicated desktop. A controller was used to issue commands, which were then translated into robot controls (e.g. up and down on the analog stick indicated the arm should move up and down, and left and right translated to moving the arm in and out). The robot continuously provided observation data (RGB-D images, joint state), which was collected at key points specified by the demonstrator via button press. These key points were roughly chosen such that linear interpolation would result in successful completion of of the task. Actions, which we specify as end effector position and orientation in the world frame, were computed using forward kinematics. Demonstrations were validated by replaying them on the robot. As an example, all collected observations for one of the *Bottle to Sink* demonstrations is shown in Figure 5.
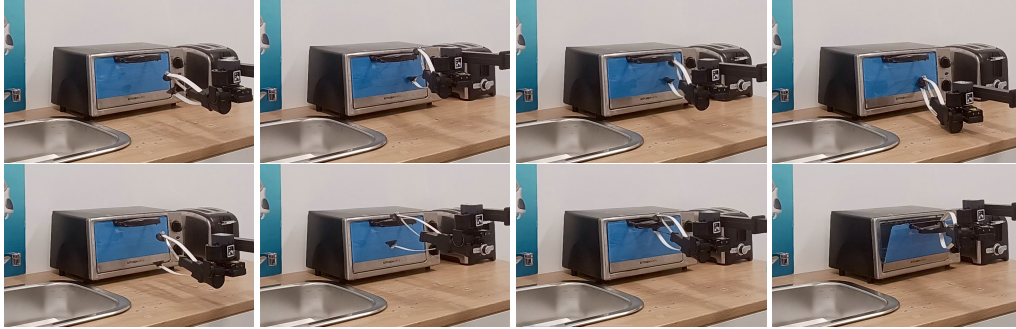
7.4 EXAMPLE GRASPS

Figure 6: An example of SANER executing a re-grasp. In the first row we see the first grasp attempt, in which the robot's gripper slips over the handle. In the second row we see SANER pulling back, lining up, and successfully executing the grasp.
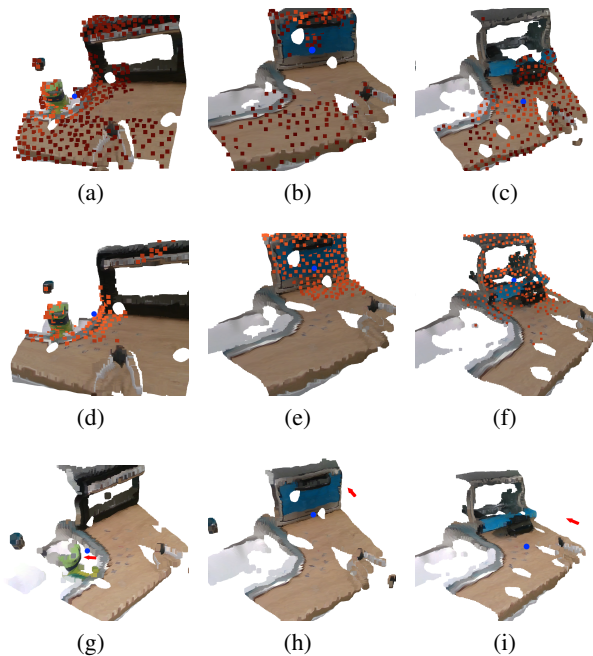
7.5 MRP ATTENTION VISUALIZATION

Figure 7: Visualizations of the attention for the MRP stream in three different settings. (a) demonstrates the MRP attending to the bottle. (b) and (c) visualize attention for the MRP by the same SANER module to two different configurations of the oven, demonstrating how ABIP attends to the handle of the oven. (d-f) represent the attention for the offset for the same settings. (g-i) represent the MRP with a blue sphere and an arrow for the predicted action.

7.6 ENVIRONMENT

RL methods collect data by taking actions in an environment. To easily adapt to the imitation learning setting, we created an RL-like environment (according to the OpenAI Gym specification) that randomly samples transitions from our recorded trajectories. Instead of returning a reward as in a normal RL environment, this environment returns the true action recorded from the demonstration. This is then used by the supervised loss described in Section 3.2.3 in place of the V-trace loss (Espeholt et al., 2018) originally used by SANE. We also created a Gym-like environment that runs the policy on the robot.

17

Formulating the imitation learning in this way has a few advantages: first, it makes training on demonstration data use the same interface as running the policy on the robot. It would also allow us to easily extend the method to an active learning setting where rewards from the environment are available. Finally, it allows us to use the baseline implementations available in CORA.

7.7 ABIP Network Architecture

7.7.1 A-PointNet

Each A-PointNet model has the following design:

1. The first set aggregation module has the following parameters:

   (a) Furthest point sampling selects 50% of points to be centers

   (b) Each center has 32 neighbors selected within a radius of 0.05m (prioritized by order in the passed in list, not proximity)

   (c) All selected neighbors are passed into a 3 layer MLP with a hidden size of 32, an output size of 32, ReLU activations, and using Instance Norm (Ulyanov et al., 2016) with no momentum or affine parameters.

   (d) The aggregation of encodings is additive.

2. The second set aggregation module has the following parameters:

   (a) Furthest point sampling selects 25% of points to be centers

   (b) Each center has 32 neighbors selected within a radius of 0.2m

   (c) All selected neighbors are passed into a 3 layer MLP with hidden sizes of 64, an output size of 128, ReLU activations, and using Instance Norm as above

   (d) The aggregation of encodings is additive

   (e) After aggregation, the embeddings are passed into another 3-layer MLP with hidden dimension 128 and output dimension 256.

3. The attention network is a 2 layer MLP with hidden dimensions of 32, and an output dimension of 1.

4. When computing the locality loss, $\bar{p}$ is detached first. This is to avoid driving $\bar{p}$ towards the unweighted center of the point cloud.

7.7.2 Policy Networks

Each policy head (position, rotation, gripper state, and completion fraction) is a 3 layer MLP with hidden dimension 32 and ReLU activation.

Inputs into the completion fraction are detached before use; this is because this estimate can be inconsistent between demonstrations, and is not necessary to complete the task.

7.8 Hyperparameters

	ABIP	No MRP Locality	No Offset Locality	Single Stream	No MRP
locality cost: MRP	100	0	100	-	-
locality cost: action prediction	10	10	0	10	10
offset dist cost	100	100	100	100	100
dual stream	yes	yes	yes	no	no
uses MRP	yes	yes	yes	yes	no

Table 4: Hyperparameters used for ablating ABIP.

		CLEAR	SANER	EWC
Common Params				
	actor learning rate	3e-4	3e-4	3e-4
	actor cost	1e5	1e5	1e5
	batch size	4	4	4
	replay ratio	6	6	-
	augmentation frames	2500	625 * 4	-
	locality cost: mrp	200	1200	100
	locality cost: offset	20	120	10
	offset dist cost	200	1200	100
SANER Params				
	critic learning rate	-	1e-4	-
	activation score cost	-	1000	-
	uncertainty cost	-	100	-
	activation scale k_{act}	-	1.0	-
	lower bound scale	-	1.0	-
	upper bound scale	-	2.0	-
	source node activation factor ($k_{s,act}$)	-	0	-
	source node upper bound factor ($k_{s,ub}$)	-	100	-
	new node activation factor ($k_{n,act}$)	-	100	-
	new node upper bound factor ($k_{n,ub}$)	-	5	-
	activation factor decay (γ_{act})	-	0.99	-
	upper bound factor decay (γ_{ub})	-	0.995	-
EWC Params				
	Per task frames	-	-	4000
	EWC λ	-	-	[1000, 10000, 100000]
	Min Frames	-	-	2000

Table 5: Hyperparameters used for the continual learning experiments.

Hyperparameters for our experiments are shown in Tables 5 and 4. Note that in the single stream ablation, we do not use the MRP stream, instead using the weighted average position from the action prediction stream as the MRP.

7.9 EVALUATION CRITERIA

Scores are reported according to the best behavior observed during the run. E.g. if the robot successfully grasps the bottle and places it in an incorrect location, then attempts a re-grasp and the bottle slips out, the robot would earn a score of 0.6 from the first interaction.

If the objects ends up in the intended location after a partial grasp (e.g. the bottle is grasped and then pushed into the sink instead of being fully picked up), we still count that as a successful placement. If the object is placed in the correct location (with release), and then perturbed (e.g. the Jello is knocked off of the oven), we still count that as a correct placement.

Pick and place tasks *Bottle to Sink* and *Bottle from Sink*, are scored according to:

1. 0.2: Partial grasp (both fingers make contact, but lose contact before raising)

2. 0.4: Full grasp, partial raise (fingers lose contact during raise)

3. 0.6: Successful raise, inaccurate placement or early release (e.g. not raised high enough)

4. 0.8: Successful placement (including opening the gripper), failure to disengage

5. 1.0: Full placement and disengagement (hand has released from the object; full retraction not required)

Task specific notes: In Bottle To Sink, getting stuck under the oven door counts as "inaccurate placement"

Oven interaction tasks Open oven and close oven are scored according to:

1. 0.2: Partial grasp, no oven door motion

2. 0.4: Partial oven door movement (¡1/4 of full motion)

3. 0.6: Half pull (1/2 open)

4. 0.8: Full door state change, unsuccessful release

5. 1.0: Full disengagement

If the robot succeeds at opening or closing the oven without the grasp specified in the demonstration, we still count that as success at the task. If the robot releases the handle while its bottom gripper is touching the table, we also count that as a success, since it's hard to open it appreciably more than that, and getting it to stay requires finesse.

7.10   SANER ACTIVATION SCORE FUNCTION

As mentioned in Section 3.3, a key goal for our score function is to be sensitive to errors approximately near the tolerance of our task and hardware, but to be less sensitive to the differences between larger errors.

We chose the $softplus$ function for its two key features: 1) an asymptote at 0, 2) no asymptote to a maximum value.

To determine the parameters to use with our score function: $softplus(\beta)(a * x + b)$, we set $\beta = 10$ and solved such that a distance of 1cm would give a score of 1, and a distance of 5cm would give a score of 0.5 This gives us $a = -12.5$ and $b = 1.13$.

For the orientation metric, we use the quaternion absolute distance and divide by 10, to scale the errors to be comparable to our position errors. This allows us to use the same $softplus$ score function as above. For the gripper, we use the absolute difference in position, and again use the same score function as above.